

# All silicon waveguide spherical microcavity coupler device

E. Xifré-Pérez,<sup>1,2</sup> J.D. Domenech,<sup>3</sup> R. Fenollosa,<sup>1,2</sup> P. Muñoz,<sup>3</sup> J. Capmany,<sup>3</sup>  
and F. Meseguer<sup>1,2,\*</sup>

<sup>1</sup>Centro de Tecnologías Físicas. Unidad Asociada CSIC-UPV, Universidad Politécnica de Valencia, Avda Tarongers s/n, 46022, Valencia, Spain

<sup>2</sup>Instituto de Ciencia de Materiales de Madrid (Consejo Superior de Investigaciones Científicas (CSIC), C/ Sor Juana Inés de la Cruz, 3, 28049, Madrid, Spain

<sup>3</sup>iTEAM Research Institute, Universidad Politécnica de Valencia, Camino de Vera s/n, Valencia, Spain  
\*fmeseg@fis.upv.es

**Abstract:** A coupler based on silicon spherical microcavities coupled to silicon waveguides for telecom wavelengths is presented. The light scattered by the microcavity is detected and analyzed as a function of the wavelength. The transmittance signal through the waveguide is strongly attenuated (up to 25 dB) at wavelengths corresponding to the Mie resonances of the microcavity. The coupling between the microcavity and the waveguide is experimentally demonstrated and theoretically modeled with the help of FDTD calculations.

© 2011 Optical Society of America

OCIS codes: (140.3945) Microcavities; (130.7408) Wavelength filtering devices.

---

## References and links

1. M. Cai, O. Painter, K. J. Vahala, and P. C. Sercel, "Fiber-coupled microsphere laser," *Opt. Lett.* **25**(19), 1430–1432 (2000).
2. J. C. Knight, N. Dubreuil, V. Sandoghdar, J. Hare, V. Lefèvre-Seguin, J. M. Raimond, and S. Haroche, "Mapping whispering-gallery modes in microspheres with a near-field probe," *Opt. Lett.* **20**(14), 1515–1517 (1995).
3. V. Lefèvre-Seguin, and S. Haroche, "Towards cavity-QED experiments with silica microspheres," *Mater. Sci. Eng. B* **48**(1-2), 53–58 (1997).
4. M. L. Gorodetsky, A. A. Savchenkov, and V. S. Ilchenko, "Ultimate Q of optical microsphere resonators," *Opt. Lett.* **21**(7), 453–455 (1996).
5. D. W. Vernooy, V. S. Ilchenko, H. Mabuchi, E. W. Streed, and H. J. Kimble, "High-Q measurements of fused-silica microspheres in the near infrared," *Opt. Lett.* **23**(4), 247–249 (1998).
6. K. J. Vahala, "Optical microcavities," *Nature* **424**(6950), 839–846 (2003).
7. A. Serpengüzel, and A. Demir, "Silicon Microspheres for Near-IR-Communication Applications," *Semicond. Sci. Technol.* **23**(6), 064009 (2008).
8. D. H. Broaddus, M. A. Foster, I. H. Agha, J. T. Robinson, M. Lipson, and A. L. Gaeta, "Silicon-waveguide-coupled high-Q chalcogenide microspheres," *Opt. Express* **17**(8), 5998–6003 (2009).
9. Y. O. Yilmaz, A. Demir, A. Kurt, and A. Serpengüzel, "Optical Channel Dropping With a Silicon Microsphere," *IEEE Photon. Technol. Lett.* **17**(8), 1662–1664 (2005).
10. V. R. Almeida, C. A. Barrios, R. R. Panepucci, and M. Lipson, "All-optical control of light on a silicon chip," *Nature* **431**(7012), 1081–1084 (2004).
11. S. Noda, A. Chutinan, and M. Imada, "Trapping and emission of photons by a single defect in a photonic bandgap structure," *Nature* **407**(6804), 608–610 (2000).
12. R. Fenollosa, F. Meseguer, and M. Tymczenko, "Silicon Colloids: from microcavities to photonic sponges," *Adv. Mater. (Deerfield Beach Fla.)* **20**(1), 95–98 (2008).
13. M. Tymczenko, PhD Thesis, March 2010.
14. E. Xifré-Pérez, R. Fenollosa, and F. Meseguer, "Low order modes in microcavities based on silicon colloids," *Opt. Express*. in press.
15. E. Xifré-Pérez, F. J. García de Abajo, R. Fenollosa, and F. Meseguer, "Photonic binding in silicon-colloid microcavities," *Phys. Rev. Lett.* **103**(10), 103902 (2009).
16. P. R. Conwell, P. W. Barber, and C. K. Rushforth, "Resonant spectra of dielectric spheres," *J. Opt. Soc. Am. A* **1**(1), 62–67 (1984).
17. C. F. Bohren, and D. R. Huffman, *Absorption and Scattering of Light by Small Particles* (John Wiley & Sons, 1998).
18. P. W. Barber, and S. C. Hill, *Light Scattering by Particles: Computational Methods* (World Scientific, 1990).
19. E. Palik, *Handbook of Optical Constants of Solids*, Vol. 1 (Academic Press, 1985).
20. F. J. García de Abajo, "Multiple Scattering of Radiation in Clusters of Dielectrics," *Phys. Rev. B* **60**(8), 6086–6102 (1999).

21. J. P. Laine, C. Tapalian, B. Little, and H. Haus, "Acceleration Sensor Based on High-Q Optical Microsphere Resonator and Pedestal Antiresonant Reflecting Waveguide Coupler," *Sens. Actuators A Phys.* **93**(1), 1–7 (2001).
  22. K. Vahala, *Optical Microcavities* (World Scientific Publishing, 2004).
  23. Y. Panitchob, G. S. Murugan, M. N. Zervas, P. Horak, S. Berneschi, S. Pelli, G. Nunzi Conti, and J. S. Wilkinson, "Whispering gallery mode spectra of channel waveguide coupled microspheres," *Opt. Express* **16**(15), 11066–11076 (2008).
  24. D. Taillaert, F. Van Laere, M. Ayre, W. Bogaerts, D. Van Thourhout, P. Bienstman, and R. Baets, "Grating couplers for coupling between optical fibers and nanophotonic waveguides," *Jpn. J. Appl. Phys.* **45**(No. 8A), 6071–6077 (2006).
  25. T. Mukaiyama, K. Takeda, H. Miyazaki, Y. Jimba, and M. Kuwata-Gonokami, "Tight-Binding Photonic Molecule Modes of Resonant Bispheres," *Phys. Rev. Lett.* **82**(23), 4623–4626 (1999).
  26. D. D. Smith, H. Chang, and K. A. Fuller, "Whispering-Gallery Mode Splitting in Coupled Microresonators," *J. Opt. Soc. Am. B* **20**(9), 1967–1974 (2003).
- 

## 1. Introduction

Whispering Gallery Mode (WGM) optical resonators and microcavities are very important devices in photonics because, due to the total internal reflection of light, the radiation is confined in very small spatial regions [1–4]. Extremely high Q factor values in microsphere type silica cavities, with a perfect spherical shape and a smooth surface, have been reported [5]. As microcavities can confine electromagnetic energy during long time [6], they are of great interest for optical processing of light, when coupled to optical fibres or waveguides [7,8]. These devices exhibit clear wavelength dependence and could, for instance, find applications as filters in optical communications systems if their spectral behavior can be tailored and controlled in the third telecommunications window. Such filtering devices have been extensively reported in the literature using other different approaches like half millimeter radius silicon spheres coupled to an optical fibre [9], ring shaped cavities coupled to Silicon-On-Insulator (SOI) waveguides [10], or 2D photonic crystal (PC) nanocavities coupled to PC waveguides [11]. In these systems cavity resonating photons can either be loaded to or extracted from the waveguide. Most high Q factor value cavities are still large in size (several tens of micrometers) since they all use low refractive index materials (SiO<sub>2</sub>) as the cavity medium. Recently, the synthesis of silicon microspheres, also called silicon colloids, was reported [12]. They are highly spherical particles with diameter from 0.5 to 5 μm and with a very smooth surface, being the roughness value around 1 nm [13]. This allows them working as photonic microcavities, with well defined Mie modes [14] in the near IR and far IR of the EM spectrum.

In this paper we present a coupler device, at telecom wavelengths (C-band), based on silicon microspheres coupled to Silicon-On-Insulator (SOI) waveguides. For this purpose, devices consisting of SOI waveguides with microspheres deposited onto them are developed and their transmitted signal is measured. These measurements are compared with a Finite Difference Time Domain (FDTD) modeling of the device.

## 2. Optical properties of silicon spherical microcavities

A very interesting characteristic of silicon microspheres is their optical confinement that makes them excellent microcavities with very-high Q-factor resonances [15]. The spectral position of the silicon microspheres resonant modes are determined by the sphere size. Both low and medium order optical modes appear in the near-infrared wavelength range for microcavity sizes between 1 and 3 μm [14]. This is an important characteristic of silicon microcavities that provide a strong light confinement in a very small volume (of the order of several cubic micrometers) for wavelengths in the telecommunication region.

Figure 1(a) shows the transmission spectrum of a single silicon microsphere, of 1.05 micrometer diameter, acquired with a Fourier Transform Infrared Spectrometer Brucker IF66/S with a spectral resolution of 1 nm by using non-polarized light [14]. The transmission dips correspond to the Mie resonance modes of the microcavity. The labels under each mode indicate the type of mode and its order. Two types of resonating modes are identified: *a* modes or transverse magnetic (TM) where the magnetic field is parallel to the surface of the

sphere, and  $b$  modes or transverse electric (TE) where the electric field is parallel to the surface of the sphere. The order of the mode is indicated by the two indices  $m, n$  that correspond to the number of maximums of the electric field in the half sphere perimeter and in the radial direction, respectively [16]. We have used the Mie theory [17,18] for fitting scattering experiments where the only fitting parameter is the microcavity diameter, and the refractive index dispersion is given by Palik [19]. The good agreement between experiment and theory is a test of the good quality of the developed silicon microcavities. Figure 1(b) shows the electric field intensity map plot for different order modes. They were calculated using a semi-analytical method based upon multiple elastic scattering of multipole expansions (MESME) [20].

The resonating characteristic of silicon microspheres is the key factor for the development of the coupler device presented here.

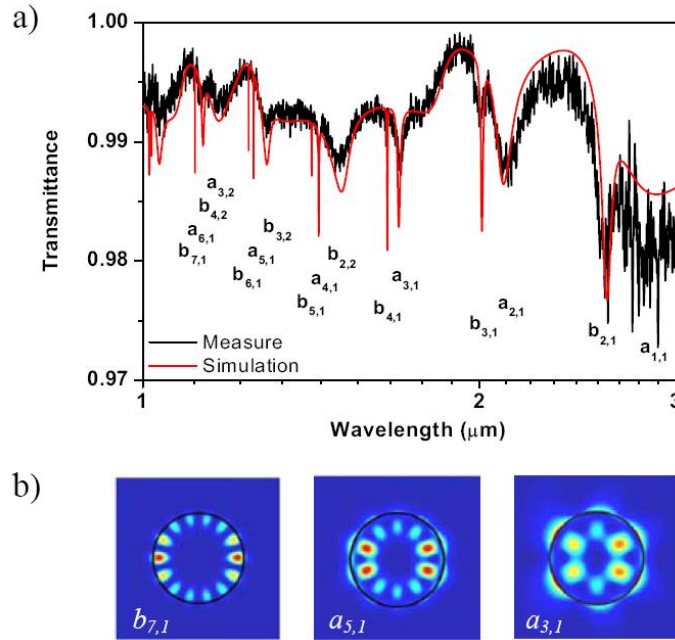


Fig. 1. Measured and calculated transmission spectra of a single silicon microcavity with diameter 1.05  $\mu\text{m}$ . The labels indicate the type and order of the resonant modes.

### 3. Theoretical analysis of the coupler device

The proposed coupler device consists of a silicon spherical microcavity placed on top of a silicon waveguide. For this purpose a calculation based on a three-dimensional finite difference time domain (3D-FDTD) method was used. As both, the sphere and the waveguide are made of silicon, the dispersive nature of refractive index value should be taken into account in the calculation. However, we have assumed a constant value for the refractive index ( $n = 3.4641$ ) since it slightly changes (less than 0.3% [19]) in the spectral region of interest (1500 nm-1600 nm). For the microsphere, an imaginary part of 0.003 has been included due to the existence of some small impurities originated during the microcavity fabrication process. The diameter of the simulated sphere is 2.49  $\mu\text{m}$ . For this size, silicon microspheres have several resonant modes in the wavelength range under study. The Si rib waveguide cross-section is 500x220  $\text{nm}^2$ , on top of a  $\text{SiO}_2$  buried oxide of 2  $\mu\text{m}$ , ensuring only TE transmission.

Firstly, the light transmitted through the waveguide is analyzed. The presence of the sphere introduces strong modifications in the transmission spectrum, especially for the

resonant modes of the microcavity. The influence of the waveguide-microcavity coupling can be observed in Fig. 2(a) where two attenuation dips are clearly observed, one around  $\lambda_1 = 1532.54$  nm and the other around  $\lambda_2 = 1586.04$  nm. For both wavelength values the guided signal is highly attenuated because the light is coupled to the microcavity. The inset of Fig. 2(a) shows the direction and polarization of the light in the coupler.

To better understand the waveguide-microcavity coupling and also to identify the type of microcavity modes coupled to the waveguide, the temporal evolution of the electric field in the coupler was studied at three different wavelength values:  $\lambda_1$  and  $\lambda_2$  that correspond to two resonant modes, and  $\lambda_3$ . For both resonant modes  $\lambda_1$  and  $\lambda_2$  the transmitted light is highly attenuated due to the strong waveguide-microcavity coupling. The electric-field distribution inside the sphere indicates that for  $\lambda_1$  the resonant mode is  $b_{10,2}$  [Fig. 2(c)] and for  $\lambda_2$  it is mode  $b_{13,1}$  [Fig. 2(d)].

It is useful comparing the waveguide-microcavity resonant modes with those of the isolated microcavity (red line in Fig. 2(a)). For the wavelength range under study, the single sphere has several  $a$  modes ( $a_{12,1}$ ,  $a_{6,3}$  and  $a_{9,2}$ ) and  $b$  modes ( $b_{13,1}$ ,  $b_{7,3}$  and  $b_{10,2}$ ). When the sphere is placed on top of the waveguide the number of resonant modes is considerably reduced. Notice that no  $a$  modes can be coupled to the waveguide but only  $b$  modes can. The reason for this effect is found in the polarization of the light: due to the design characteristics of the waveguide, only TE polarization propagates along the waveguide. Then, only  $b$  modes can be excited [15] since the resonant plane is tangent to the guide (see top Fig. 2(b)). From the calculated transmission spectrum of the coupler device, only the modes  $b_{10,2}$  (at  $\lambda_1$ ) and  $b_{13,1}$  (at  $\lambda_2$ ) of the isolated microcavity do couple to the waveguide but  $b_{7,3}$  does not. Also, the temporal evolution of the electric field in the coupler for the wavelength range where mode  $b_{7,3}$  should exist show a non-resonant behavior as observed for  $\lambda_3$  in Fig. 2(e). For this wavelength the light does not couple to the sphere and it travels to the end of the waveguide being barely attenuated. The reason for this different behavior lies in the electric field distribution of the different modes. The electric field map plot of modes  $b_{13,1}$  and  $b_{10,2}$  are concentrated near the microcavity interface and therefore they feel the presence of the waveguide. On the contrary, the electric field map plot of the  $b_{7,3}$  mode is concentrated deep inside the microcavity [Fig. 2(f)], at a radial distance from the surface that hinders the light coupling to the waveguide.

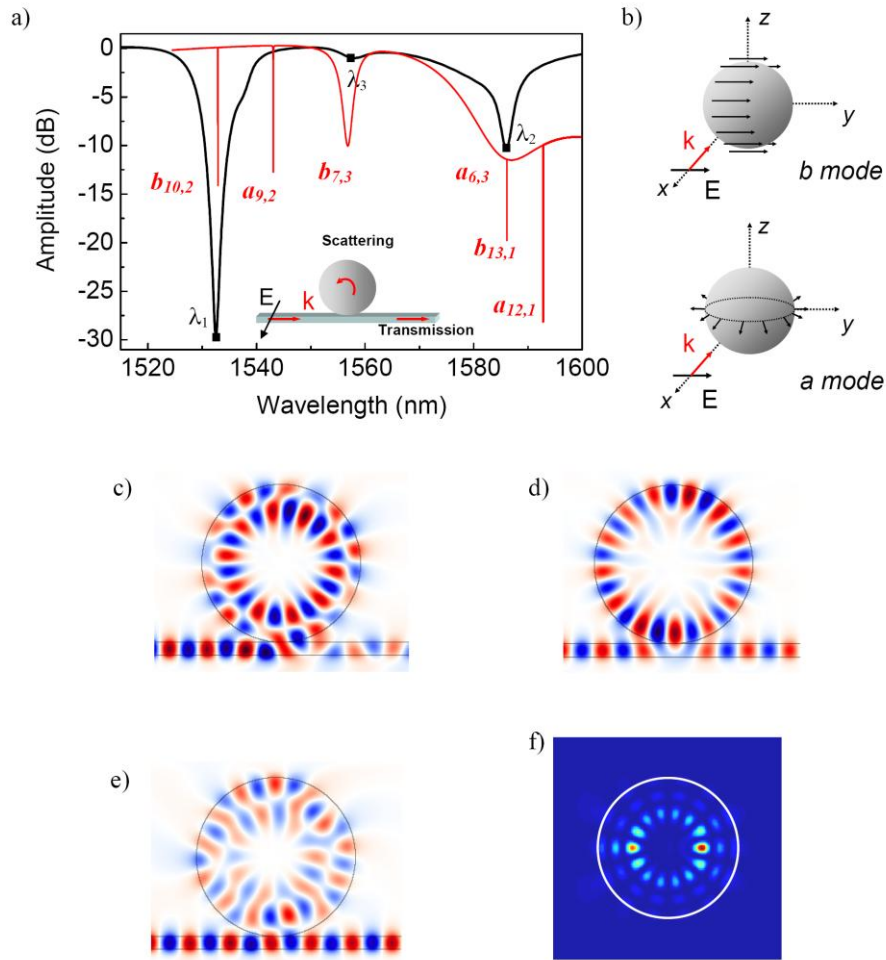


Fig. 2. (a) Calculated transmission of the coupler device consisting of a waveguide with a silicon microcavity placed on top (black line). The diameter of the microsphere is  $2.49 \mu\text{m}$ . The red line is the transmission spectrum of the single microsphere and the red labels indicate the type and order of the modes. The inset indicates the direction of the propagation and the polarization for the light in the coupler. The waveguide is parallel to the  $x$  direction (b) Resonant plane of  $b$  (top) and  $a$  (bottom) modes. c-e) Snapshot of the temporal evolution of the electric field distribution in the coupler calculated by 3D-FDTD for the resonant modes of the sphere: (c)  $b_{10,2}$  ( $\lambda_1$ ), (d)  $b_{13,1}$  ( $\lambda_2$ ) and (e) for a non-resonant wavelength ( $\lambda_3$ ) (f) Electric-field intensity distribution for the isolated microcavity mode  $b_{7,3}$ . The surface of the microcavity is indicated with the white circle.

By comparing the modes  $b_{13,1}$  and  $b_{10,2}$  for the single sphere and for the sphere in the coupler a dramatic reduction of the Q-factor is observed as a result of the coupling between the waveguide and the microcavity [21]. Nevertheless, the waveguide-microcavity coupling efficiency strongly depends on the waveguide-sphere separation in the direction normal to the surface of the waveguide so an increase of the Q-factor would be possible by optimizing this distance [22,23].

#### 4. Experimental results and discussion

##### 4.1. Fabrication of the coupler device

The silicon waveguides were produced on a standard SOITEC wafer by deep UV lithography in an ePIXfab platform. Their length is about 3 mm, their cross section is  $500 \times 220 \text{ nm}^2$  as

outlined above, and at both ends a grating coupler is used so that light can be easily in/out coupled to/from the waveguides [24]. Both, waveguides and grating couplers were designed for transmitting only TE polarized light around 1550 nm. Light from a tunable laser ANDO AQ4321D was coupled to the waveguide and the transmitted signal was measured by a synchronized spectrum analyzer ANDO AQ6317C. The schematic of the experimental setup is shown in Fig. 3.

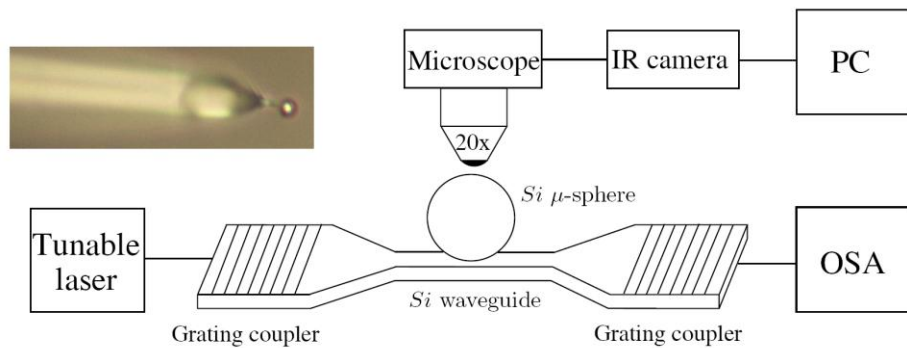


Fig. 3. Schematic of the experimental setup. Inset: image of one of the needle shaped tools fabricated and used for the pick-and-place operation of the sphere. A silicon microsphere can also be observed at the tip of the tool.

Silicon microspheres are obtained by chemical vapor deposition means, using di-silane as a precursor gas [12]. This method allows synthesizing amorphous and poly-crystalline silicon microspheres. For this work, poly-crystalline microspheres were chosen. Because the as-grown samples consist of a substrate with many isolated and clustered spheres, with sizes from 0.5 to 5 micrometers, we performed a selection of spheres (within the limited resolution of the optical microscope at 1000x magnification) having a diameter from 2.0 to 2.5 micrometers approximately. The size is a very important parameter as it determines the spectral position of the resonant modes that must be within the transmission wavelength range of the waveguide. Optical transmittance measurements were performed on selected microspheres, one by one, in a wide wavelength range, from 1 to 3 micrometers (see Fig. 1). This allows identifying the resonant modes and precisely determining the sphere diameter by fitting the measured signal to Mie theory [12]. Therefore, only those microspheres having resonant modes within the transmission range of the waveguides were considered as candidates for developing the coupler.

Finally, the candidate microspheres were placed on top of the silicon waveguides with the help of micromanipulation techniques. Different needle-shaped tools were fabricated for the pick-and-place operation and also for the fine positioning of the spheres on the waveguides (inset of Fig. 3). The inset of Fig. 4 shows the optical microscopy image (top view) of the microsphere on top of the waveguide. The diameter of the sphere, determined by the procedure described above, is 2.49  $\mu\text{m}$ , the same diameter used for the theoretical study in section 3.

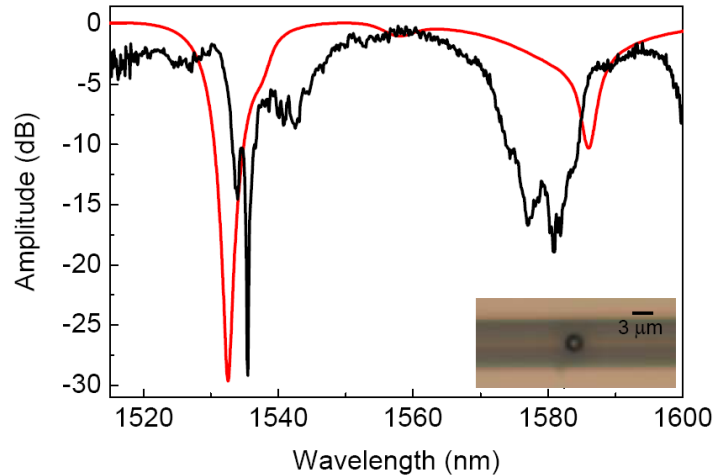


Fig. 4. Measured transmission spectrum of the coupler device (black curve) and 3D-FDTD calculated transmission (red curve). Inset: Microscope image (top view) of the silicon microsphere placed on top of the waveguide. The diameter of the microsphere is  $2.49\ \mu\text{m}$ .

#### 4.2. Transmission measurements

The measured transmission spectrum of the silicon waveguide with a  $2.49\ \mu\text{m}$  diameter microsphere placed on top is presented in Fig. 4 (black curve) and compared to the calculated transmission spectrum (red curve). Two attenuation dips corresponding to modes  $b_{10,2}$  and  $b_{13,1}$  are identified around  $1534\ \text{nm}$  and  $1580\ \text{nm}$  respectively. The attenuation peak for mode  $b_{10,2}$  is much narrower and deeper than the peak for mode  $b_{13,1}$  as expected from the simulation. It should be stressed the strong attenuation of the signal for mode  $b_{10,2}$ , of about  $30\ \text{dB}$ .

We can also observe that the coupled modes  $b_{10,2}$  and  $b_{13,1}$  split into two dips each, an effect not observed in the simulation. This mode splitting may be caused by the break of the mode degeneracy [25,26]. As the micromanipulation technique does not guarantee a precise control of the position of the microcavity on the waveguide, a slight off axis displacement of the sphere (in the lateral direction) would modify the coupled resonances as observed in Fig. 4. Finally, the shift of the wavelength position can be due to the error determining the microcavity size, since the above mentioned method (see Section 2) determines the diameter of the sphere with an accuracy of approximately ten nanometers.

#### 4.3. Imaging the scattered light

The results presented above have demonstrated the light coupling between the waveguide and the microcavity for resonant mode wavelengths. The light is trapped inside the sphere and then scattered away. The detection of this scattered light is possible with the help of an infrared camera-microscope objective system placed over the coupler as shown in Fig. 3.

Figure 5 (Media 1) shows the transmission spectrum of a waveguide-microcavity coupler device, whereas the insets show the IR image of the microsphere for the three different wavelength values indicated by the vertical red line. The transmission spectrum shows two resonant modes of the sphere,  $b_{10,2}$  and  $b_{13,1}$ , the same ones analyzed in the previous sections.

When the wave-guided light couples to the microcavity the transmission shows a minimum and simultaneously the IR camera detects light coming out from the cavity (left and right inset panels of Fig. 5, Media 1). The different Q-factors of the modes are perceived in the different intensity of the scattered light, higher for the mode around  $\lambda_1 = 1548\ \text{nm}$  than for the mode around  $\lambda_2 = 1607\ \text{nm}$ . This is consistent with the measured transmission spectrum as the attenuation for  $\lambda_1$  is higher than for  $\lambda_2$ . On the contrary, for non-resonant wavelengths, the

light is not confined inside the sphere and therefore no scattering light is detected (center image of Fig. 5, [Media 1](#)).

The scattered light detected here by the IR camera for the resonant wavelengths can also be collected by a fiber optic and processed for applications in communications as drop and notch filters and multiplexers.

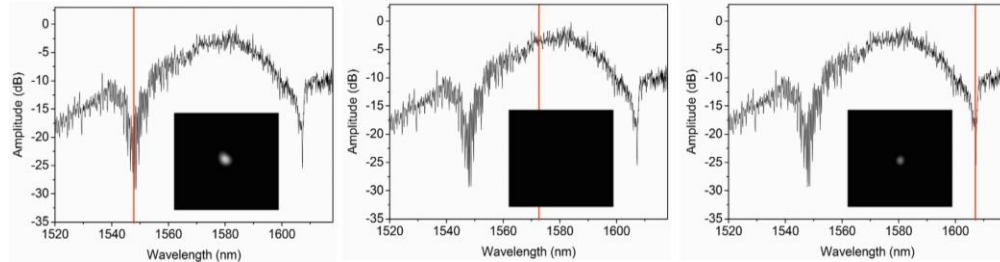


Fig. 5. Transmission spectrum of the coupler device for a silicon microsphere with diameter 2.5  $\mu\text{m}$ . The inset shows the IR camera image of the light scattered by the microcavity for the wavelength indicated by the red line. Two modes are observed:  $b_{10,2}$  (left) and  $b_{13,1}$  (right). A non-resonant wavelength is also presented (center). Video online ([Media 1](#)).

## 5. Conclusions

A coupler device based on silicon spherical microcavities has been proposed for the telecommunication region. The transmittance, coupling and confinement of light in the coupler have been theoretically and experimentally demonstrated. We have shown the discriminating coupling of low order  $b$  modes for  $TE$  polarized light and the splitting effect of the attenuation peaks. The Q-factor of the coupler modes can be increased by slightly separating the microcavity from the waveguide, thus taking more advantage of the very-high Q-factor modes of silicon microcavities. The light scattered by the microcavity for the resonant modes has been detected, being its intensity consistent with the transmission spectrum measured for the coupler. This scattered light can also be collected by a fiber optic and it can be further processed. The coupler device presented here can extend the range of applications for silicon microcavities/SOI technology based devices in optical filtering and signal processing.

## Acknowledgements

The authors wish to acknowledge financial support from projects FIS2009-07812; Consolider Nanolight.es 2007/0046 and N° 1841; the Spanish Education and Science Ministry, TEC2008-06145; the Generalitat Valenciana, project PROMETEO/2008/092 and PROMETEO/2010/043; and project Apoyo a la investigación 2009 from Universidad Politecnica de Valencia, n° reg. 4325. E. Xifré-Pérez acknowledges the financial support from the program Juan de la Cierva (Spanish Ministerio de Educación y Ciencia). J. D. Doménech acknowledges the FPI research grant BES-2009-018381. Finally we thank Prof. J. Garcia de Abajo for providing us with the MESME theoretical program we have used in the calculation of electric field intensity distribution of the Mie modes.